Supplemental Materials

Molecular Biology of the Cell

Saito et al.

Figure S1

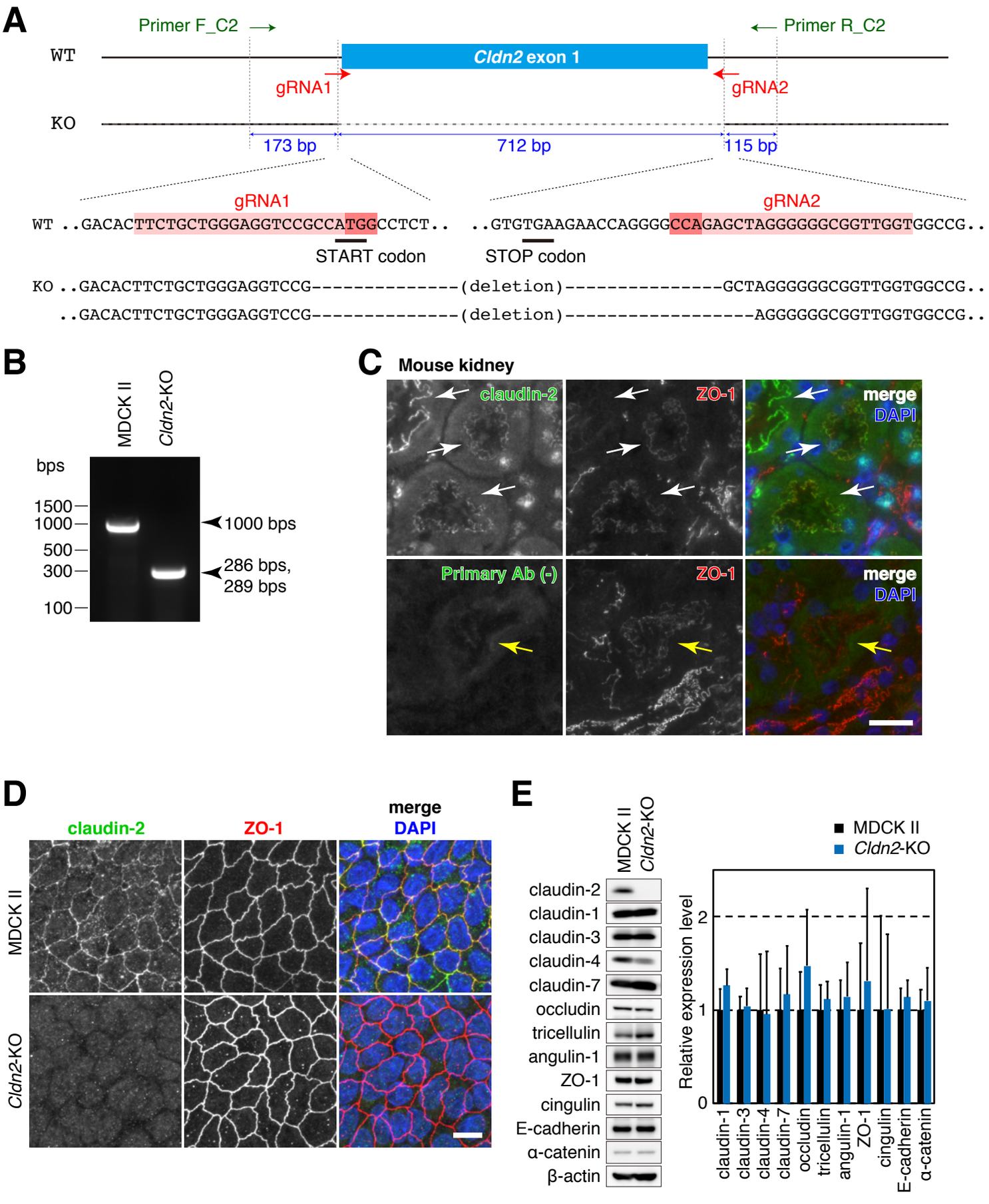
A
Primer F_C2
Primer R_C2
WT
Cldn2 exon 1
gRNA1
gRNA2
KO
173 bp
712 bp
115 bp
gRNA1
gRNA2
WT ..GACACTTCTGCTGGGAGGTCCGCCATGGCCTCT..
..GTGTGAAGAACCAGGGGCCAGAGCTAGGGGGGCGGTTGGTGGCCG..
START codon
STOP codon
KO ..GACACTTCTGCTGGGAGGTCCG----------(deletion)----------GCTAGGGGGGCGGTTGGTGGCCG..
..GACACTTCTGCTGGGAGGTCCG----------(deletion)----------AGGGGGGCGGTTGGTGGCCG..
B
MDCK II
Cldn2-KO
bps
1500
1000
500
300
100
1000 bps
286 bps,
289 bps
C
Mouse kidney
claudin-2
ZO-1
merge
DAPI
Primary Ab (-)
ZO-1
merge
DAPI
D
claudin-2
ZO-1
merge
DAPI
MDCK II
Cldn2-KO
E
MDCK II
Cldn2-KO
claudin-2
claudin-1
claudin-3
claudin-4
claudin-7
occludin
tricellulin
angulin-1
ZO-1
cingulin
E-cadherin
α-catenin
β-actin
MDCK II
Cldn2-KO
Relative expression level
0
1
2
claudin-1
claudin-3
claudin-4
claudin-7
occludin
tricellulin
angulin-1
ZO-1
cingulin
E-cadherin
α-catenin

Figure S1. Generation of *Cldn2*-KO cells derived from MDCK II cells

(A) Genomic structure of canine *Cldn2* gene and schema of knockout strategy.

(B) Genomic PCR of parental MDCK II cells and *Cldn2*-KO MDCK II cells ("Ctrl cells").

(C) Characterization of rat anti-claudin-2 mAb (2D7) used for immunostaining. Frozen sections of the mouse kidney were stained with (upper panels) or without (lower panels) rat anti-claudin-2 mAb (green) together with rabbit anti-ZO-1 pAb (red) and DAPI (blue). Note that claudin-2 is positive at the cell-cell junctions of the proximal tubules (white arrows) in the kidney and that treatment with anti-rat secondary antibody alone does not stain the proximal tubule (yellow arrows). Scale bar, 20 μm.

(D) Immunofluorescence staining of parental MDCK II cells and *Cldn2*-KO MDCK II cells using rat anti-claudin-2 mAb (green), rabbit anti-ZO-1 pAb (red) and DAPI (blue). Scale bar, 20 μm.

(E) Immunoblotting analysis of *Cldn2*-KO MDCK II cells with rabbit anti-claudin2 pAb, rabbit anti-claudin-1 pAb, rabbit anti-claudin-3 pAb, mouse anti-claudin-4 mAb, rabbit anti-claudin7 pAb, rabbit anti-occludin pAb, rabbit anti-tricellulin mAb, rabbit anti-angulin-1 pAb, rat anti-ZO-1 mAb, mouse anti-cingulin mAb, mouse anti-E-cadherin mAb, rabbit anti-α-catenin mAb and mouse anti-β-actin mAb. β-actin serves as a reference control. Quantification of the bands from five independent experiments are shown. The band intensities were normalized based on the corresponding β-actin band and fold changes of the expression level from the parental MDCK II cells are shown. None of the proteins examined differed significantly in expression levels by Welch's t-test.

Figure S2

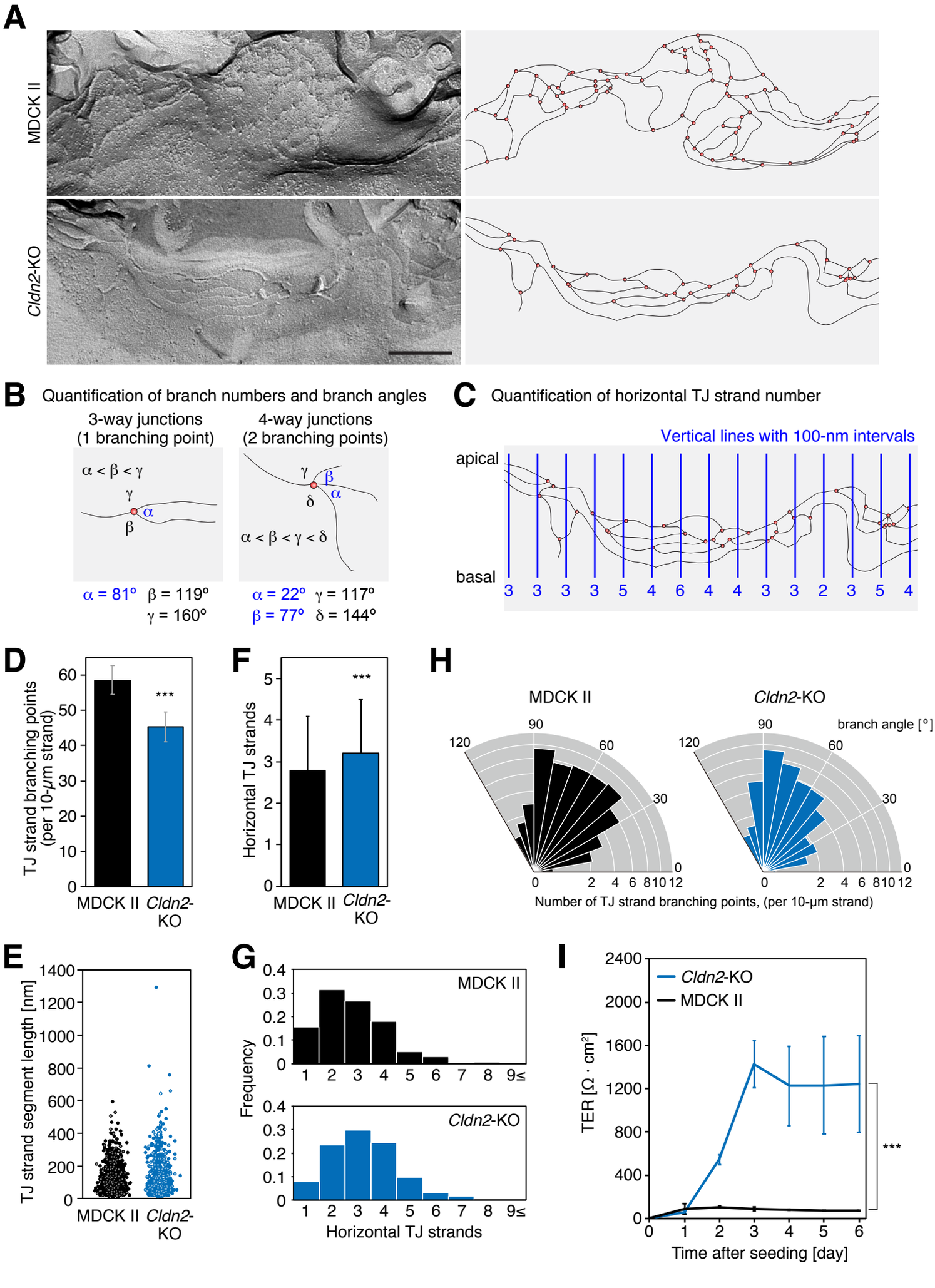
A
MDCK II
Cldn2-KO
B
Quantification of branch numbers and branch angles
3-way junctions
(1 branching point)
4-way junctions
(2 branching points)
α < β < γ
α = 81° β = 119°
γ = 160°
α < β < γ < δ
α = 22° γ = 117°
β = 77° δ = 144°
C
Quantification of horizontal TJ strand number
Vertical lines with 100-nm intervals
apical
basal
3 3 3 3 5 4 6 4 4 3 3 2 3 5 4
D
TJ strand branching points (per 10-μm strand)
***
MDCK II
Cldn2-KO
F
Horizontal TJ strands
***
MDCK II
Cldn2-KO
H
MDCK II
Cldn2-KO
branch angle [°]
Number of TJ strand branching points, (per 10-μm strand)
E
TJ strand segment length [nm]
MDCK II
Cldn2-KO
G
MDCK II
Cldn2-KO
Frequency
Horizontal TJ strands
I
Cldn2-KO
MDCK II
TER [Ω · cm²]
***
Time after seeding [day]

Figure S2. *Cldn2*-KO cells have a less complex TJ strand network and an improved barrier for ions compared with parental MDCK II cells

(A) Freeze-fracture replicas of parental MDCK II cells (upper panel) and *Cldn2*-KO MDCK II cells (lower panel). TJ strands on the replica images were traced and the network organization is shown (right panels). Note that the TJ strands of *Cldn2*-KO cells are continuous and almost all particles are found on the protoplasmic face of the replica in contrast to the discontinuous TJ strands in the parental MDCK II cells. Scale bar, 200 nm.

(B) Quantification method for branching points (junction points) and branch angles of TJ strand. In the three-way junctions, three angles were measured, and the smallest angle was recorded. Four-way junctions were regarded as two three-way junctions, and two smallest angles were recorded.

(C) Quantification method for the number of horizontal TJ strands. The TJ strands on the replica images were traced. Apical-to-basal lines with 100-nm intervals were drawn and the number of TJ strands crossing the vertical lines was counted.

(D) Number of TJ strand branching points (junction points) in the parental MDCK II cells and *Cldn2*-KO cells. Number of three-way branching points were divided by the total length of TJ strands (>100 μm from more than 20 images for each clone). Error bars indicate 95% confidence interval. *** $p = 4.71 \times 10^{-9}$ in Poisson's exact rate test.

(E) The lengths of TJ strand segments are plotted. Observed TJ strand segments are classified into three categories: closed segment (branching point-to-branching point; circles filled with dark color); semi-open segment (branching point-to-endpoint; circles filled with light color) and open segment (endpoint-to-endpoint; open circles).

(F) Number of horizontal TJ strands of the parental MDCK II cells and *Cldn2*-KO cells. n = 361 (parental MDCK II cells), 188 (*Cldn2*-KO cells). *** $p = 3.36 \times 10^{-4}$ in Welch's t-test.

(G) Distributions of the horizontal TJ strand number in the parental MDCK II cells and *Cldn2*-KO cells are plotted.

(H) The branch angles of TJ strand. The angles measured by the method shown in (B) were plotted in polar area plots, in which the area of each sector is proportional to the value.

(I) TER measurement of *Cldn2*-KO MDCK II cells. Note that the *Cldn2*-KO cells have a much tighter permeability barrier compared with the parental MDCK II cells. Data are shown as mean ± SEM. n = 9. *** $p = 2.01 \times 10^{-5}$ in Welch's t-test of the TER values on Day 6.

Figure S3

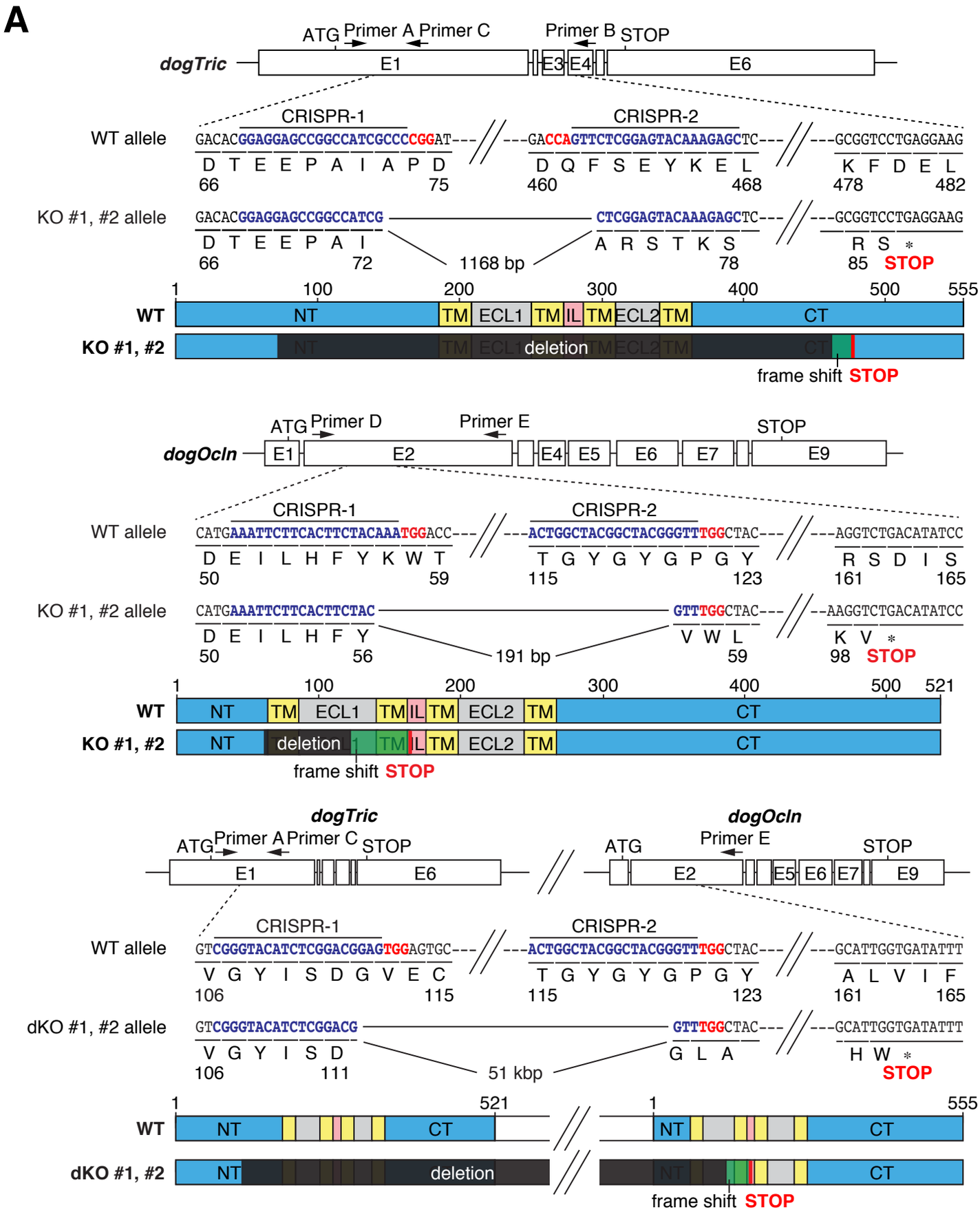
A
dogTric
ATG
Primer A
Primer C
Primer B
STOP
E1
E3
E4
E6
CRISPR-1
CRISPR-2
WT allele
GACACGGAGGAGCCGGCCATCGCCCCGGAT---
---GACCAGTTCTCGGAGTACAAAGAGCTC---
---GCGGTCCTGAGGAAG
D T E E P A I A P D
66
75
D Q F S E Y K E L
460
468
K F D E L
478
482
KO #1, #2 allele
GACACGGAGGAGCCGGCCATCG
CTCGGAGTACAAAGAGCTC---
---GCGGTCCTGAGGAAG
D T E E P A I
66
72
1168 bp
A R S T K S
78
R S *
85
STOP
1
100
200
300
400
500
555
WT
NT
TM
ECL1
TM
IL
TM
ECL2
TM
CT
KO #1, #2
deletion
frame shift
STOP
dogOcln
ATG
Primer D
Primer E
STOP
E1
E2
E4
E5
E6
E7
E9
CRISPR-1
CRISPR-2
WT allele
CATGAAATTCTTCACTTCTACAAATGGACC---
---ACTGGCTACGGCTACGGGTTTGGCTAC---
---AGGTCTGACATATCC
D E I L H F Y K W T
50
59
T G Y G Y G P G Y
115
123
R S D I S
161
165
KO #1, #2 allele
CATGAAATTCTTCACTTCTAC
GTTTGGCTAC---
--AAGGTCTGACATATCC
D E I L H F Y
50
56
191 bp
V W L
59
K V *
98
STOP
1
100
200
300
400
500
521
WT
NT
TM
ECL1
TM
IL
TM
ECL2
TM
CT
KO #1, #2
NT
deletion
TM
IL
TM
ECL2
TM
CT
frame shift
STOP
dogTric
dogOcln
ATG
Primer A
Primer C
STOP
E1
E6
ATG
Primer E
STOP
E2
E5
E6
E7
E9
CRISPR-1
CRISPR-2
WT allele
GTCGGGTACATCTCGGACGGAGTGGAGTGC---
---ACTGGCTACGGCTACGGGTTTGGCTAC---
---GCATTGGTGATATTT
V G Y I S D G V E C
106
115
T G Y G Y G P G Y
115
123
A L V I F
161
165
dKO #1, #2 allele
GTCGGGTACATCTCGGACG
GTTTGGCTAC---
---GCATTGGTGATATTT
V G Y I S D
106
111
51 kbp
G L A
H W *
STOP
1
521
1
555
WT
NT
CT
NT
CT
dKO #1, #2
NT
deletion
NT
CT
frame shift
STOP
B
Tric-KO
Ctrl
#1
#2
Primer A-B
Primer A-C
Ocln-KO
Ctrl
#1
#2
Primer D-E
Tric/Ocln-dKO
Ctrl
#1
#2
Primer A-E
Primer A-C

Figure S3. Genomic DNA structure of *Tric*-KO, *Ocln*-KO, and *Tric*/*Ocln*-dKO cells
(A) Genomic structure of dog *Tric* and *Ocln* loci and protein structures of dog tricellulin and occludin are shown. gRNAs used for the generation of KO cells are shown and PAM sequences are depicted in red. Genomic sequencing of *Tric*-KO, *Ocln*-KO, and *Tric*/*Ocln*-dKO cells revealed frameshift mutations. In *Tric*-KO cells, 1168-bp deletion was detected from N-terminal cytoplasmic region (NT) to C-terminal cytoplasmic region (CT) in both alleles of clones #1 and #2. In *Ocln*-KO cells, 191-bp deletion was detected from NT to the first extracellular loop (ECL1) region in both alleles of clones #1 and #2. In the *Tric*/*Ocln*-dKO cells, approximately 51 kbp deletion was detected from the NT of tricellulin to the intracellular loop (IL) region of occludin in both alleles of clones #1 and #2.
(B) Genomic PCR of WT and KO cells. Primer sequences are listed in Table S2.

Figure S4

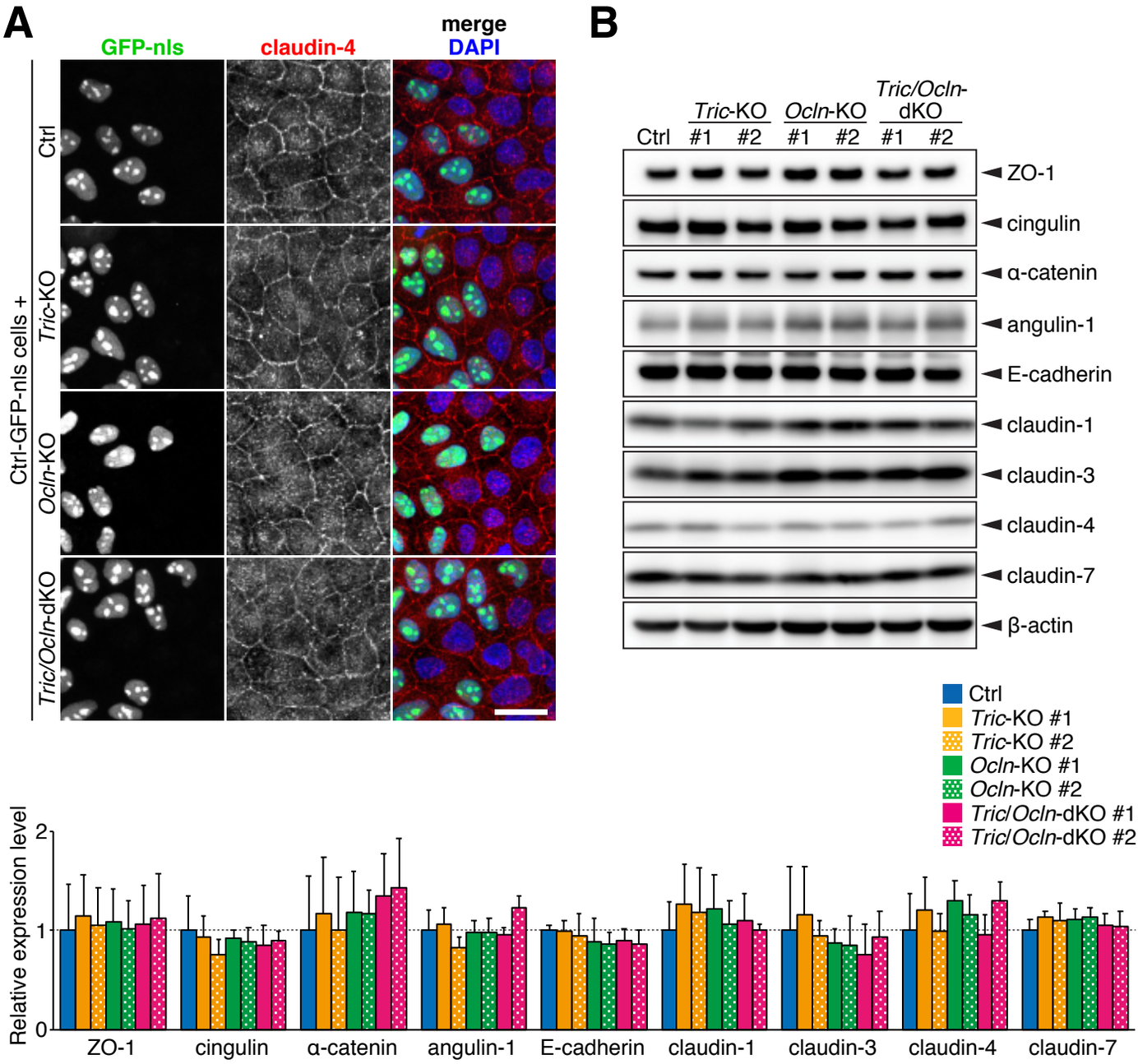
A
GFP-nls
claudin-4
merge
DAPI
Ctrl-GFP-nls cells +
Ctrl
Tric-KO
Ocln-KO
Tric/Ocln-dKO
B
Tric-KO
Ocln-KO
Tric/Ocln-dKO
Ctrl
#1
#2
#1
#2
#1
#2
ZO-1
cingulin
α-catenin
angulin-1
E-cadherin
claudin-1
claudin-3
claudin-4
claudin-7
β-actin
Ctrl
Tric-KO #1
Tric-KO #2
Ocln-KO #1
Ocln-KO #2
Tric/Ocln-dKO #1
Tric/Ocln-dKO #2
Relative expression level
0
1
2
ZO-1
cingulin
α-catenin
angulin-1
E-cadherin
claudin-1
claudin-3
claudin-4
claudin-7

Figure S4. *Tric/Ocln*-dKO cells show no consistent changes in the expression of TJ or AJ proteins

(A) Ctrl-GFP-nls cells were mixed and co-cultured with Ctrl, *Tric*-KO, *Ocln*-KO, or *Tric*/*Ocln*-dKO cells. Cells were stained with mouse anti-claudin-4 mAb (red) together with DAPI (blue). The nuclear GFP (green) was detected in the green channel. Scale bars, 20 μm.

(B) Immunoblotting of the total cell lysates of Ctrl, *Tric*-KO, *Ocln*-KO and *Tric*/*Ocln*-dKO cells with rat anti-ZO-1 mAb, mouse anti-cingulin mAb, rabbit anti-α-catenin mAb, rabbit anti-angulin-1 pAb, rabbit anti-E-cadherin mAb, rabbit anti-claudin-1 pAb, rabbit anti-claudin-3 pAb, mouse anti-claudin-4 mAb, rabbit anti-claudin-7 pAb and mouse anti-β-actin mAb. β-actin served as a reference control. Quantification of the bands from four independent experiments are shown. The band intensities were normalized based on the corresponding β-actin band and fold changes of the expression levels from the Ctrl cells are shown. None of the proteins examined differed significantly in expression levels according to Welch's t-test with Bonferroni's correction.

Figure S5

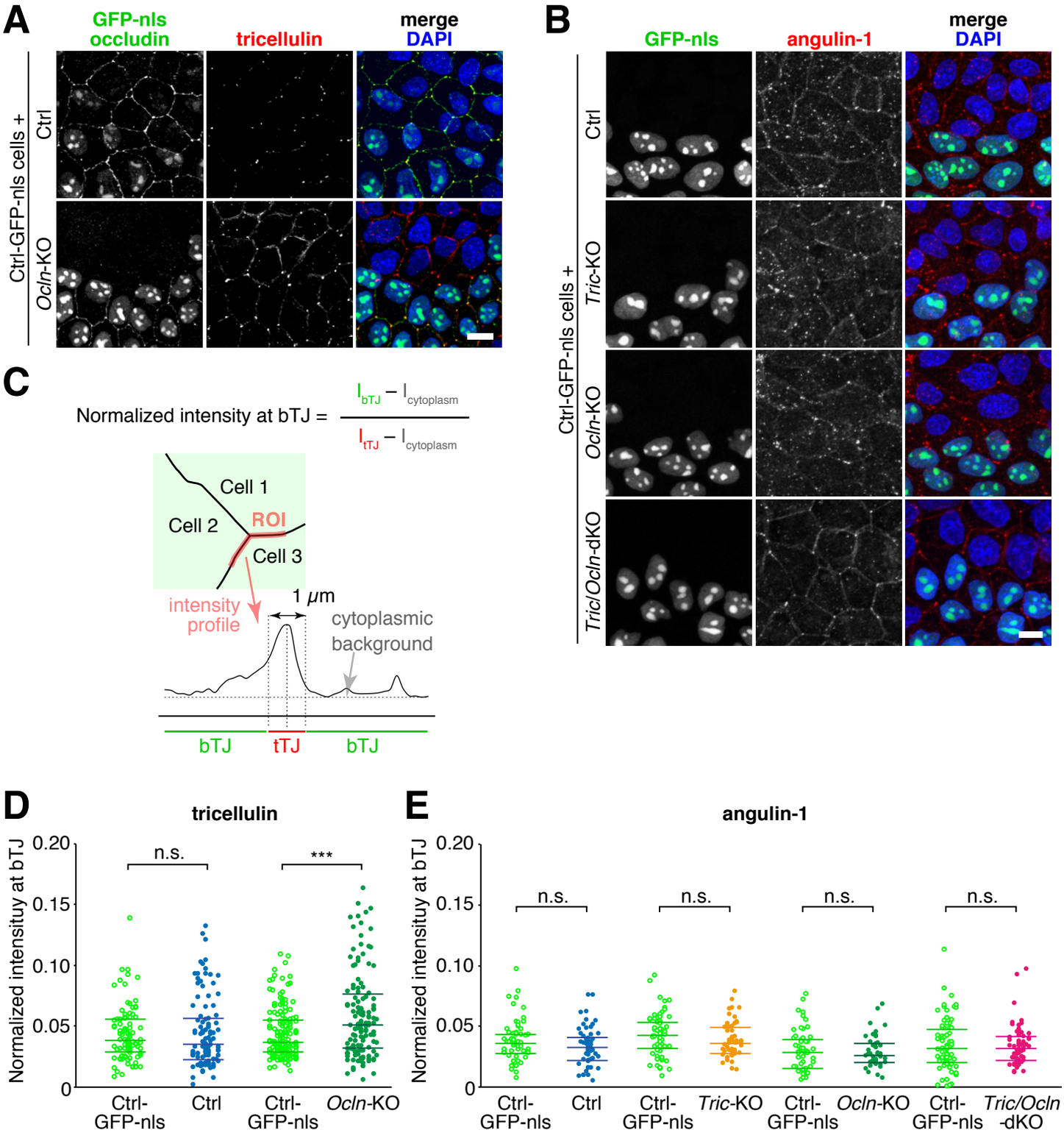
A
GFP-nls
occludin
tricellulin
merge
DAPI
Ctrl-GFP-nls cells +
Ctrl
Ocln-KO
B
GFP-nls
angulin-1
merge
DAPI
Ctrl-GFP-nls cells +
Ctrl
Tric-KO
Ocln-KO
Tric/Ocln-dKO
C
Normalized intensity at bTJ = (I bTJ – I cytoplasm) / (I tTJ – I cytoplasm)
Cell 1
Cell 2
Cell 3
ROI
1 μm
intensity profile
cytoplasmic background
bTJ
tTJ
bTJ
D
tricellulin
Normalized intensituy at bTJ
0.20
0.15
0.10
0.05
0
n.s.
***
Ctrl-GFP-nls
Ctrl
Ctrl-GFP-nls
Ocln-KO
E
angulin-1
Normalized intensituy at bTJ
0.20
0.15
0.10
0.05
0
n.s.
n.s.
n.s.
n.s.
Ctrl-GFP-nls
Ctrl
Ctrl-GFP-nls
Tric-KO
Ctrl-GFP-nls
Ocln-KO
Ctrl-GFP-nls
Tric/Ocln-dKO

Figure S5. *Ocln*-KO leads to mislocalization of tricellulin, but not angulin-1, at bicellular TJ

(A) Ctrl or *Ocln*-KO #1 cells were mixed and co-cultured with Ctrl-GFP-nls cells. Cells were immunostained with rat anti-occludin mAb (green) and rabbit anti-tricellulin mAb (red). The nuclear GFP signal of Ctrl-GFP-nls cells was detected together with occludin signal in the green channel. Scale bar, 20 μm.

(B) Ctrl, *Tric*-KO #1, *Ocln*-KO #1 or *Tric*/*Ocln*-dKO #1 cells were mixed and co-cultured with Ctrl-GFP-nls cells. Cells were immunostained with rabbit anti-angulin-1 pAb (red). The nuclear GFP signal of Ctrl-GFP-nls cells were detected in the green channel. Scale bar, 20 μm.

(C) Quantification method of tricellular confinement of tricellulin or angulin-1. The fluorescence intensities at bicellular junctions (I_{bTJ}) were normalized to the intensity at the adjacent tricellular junction (I_{tTJ}). The background signal of cytoplasmic region ($I_{cytoplasm}$) was subtracted.

(D) Quantification of tricellular confinement of tricellulin in the *Ocln*-KO cells. The relative fluorescence intensities of tricellulin at bicellular TJs were plotted and 25, 50 and 75 percentiles are shown (lines). n = 90 and 102 (Ctrl-GFP-nls vs Ctrl, p = 0.669), 153 and 138 (Ctrl-GFP-nls vs *Ocln*-KO #1, $p = 2.07 \times 10^{-5}$). ***$p < 0.001$; n.s., $p \geq 0.05$ in Welch's t-test.

(E) Quantification of tricellular confinement of angulin-1 in the *Tric*-KO, *Ocln*-KO and *Tric*/*Ocln*-dKO cells. 25, 50 and 75 percentiles are shown (lines). n=39-75. The relative intensities of angulin-1 at bTJs in any clones were not significantly different with those of Ctrl-GFP-nls cells (Welch's t-test).

Figure S6

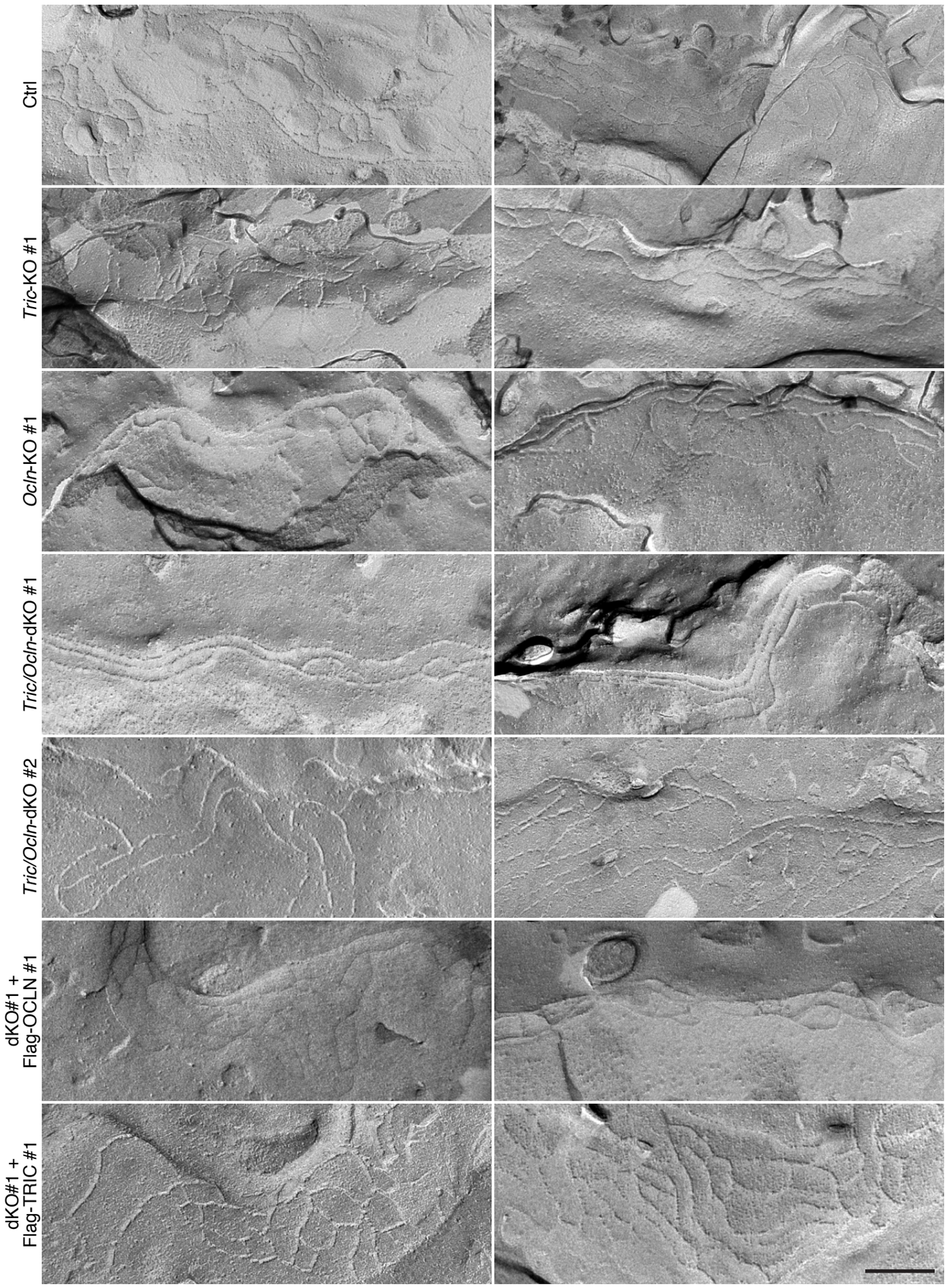

Figure S6. Freeze-fracture replica electron microscopy images of Ctrl, *Tric*-KO, *Ocln*-KO, *Tric*/*Ocln*-dKO #1 and #2, dKO#1+Flag-OCLN #1 and dKO#1+Flag-TRIC #1 cells. Scale bar, 200 μm.

Figure S7

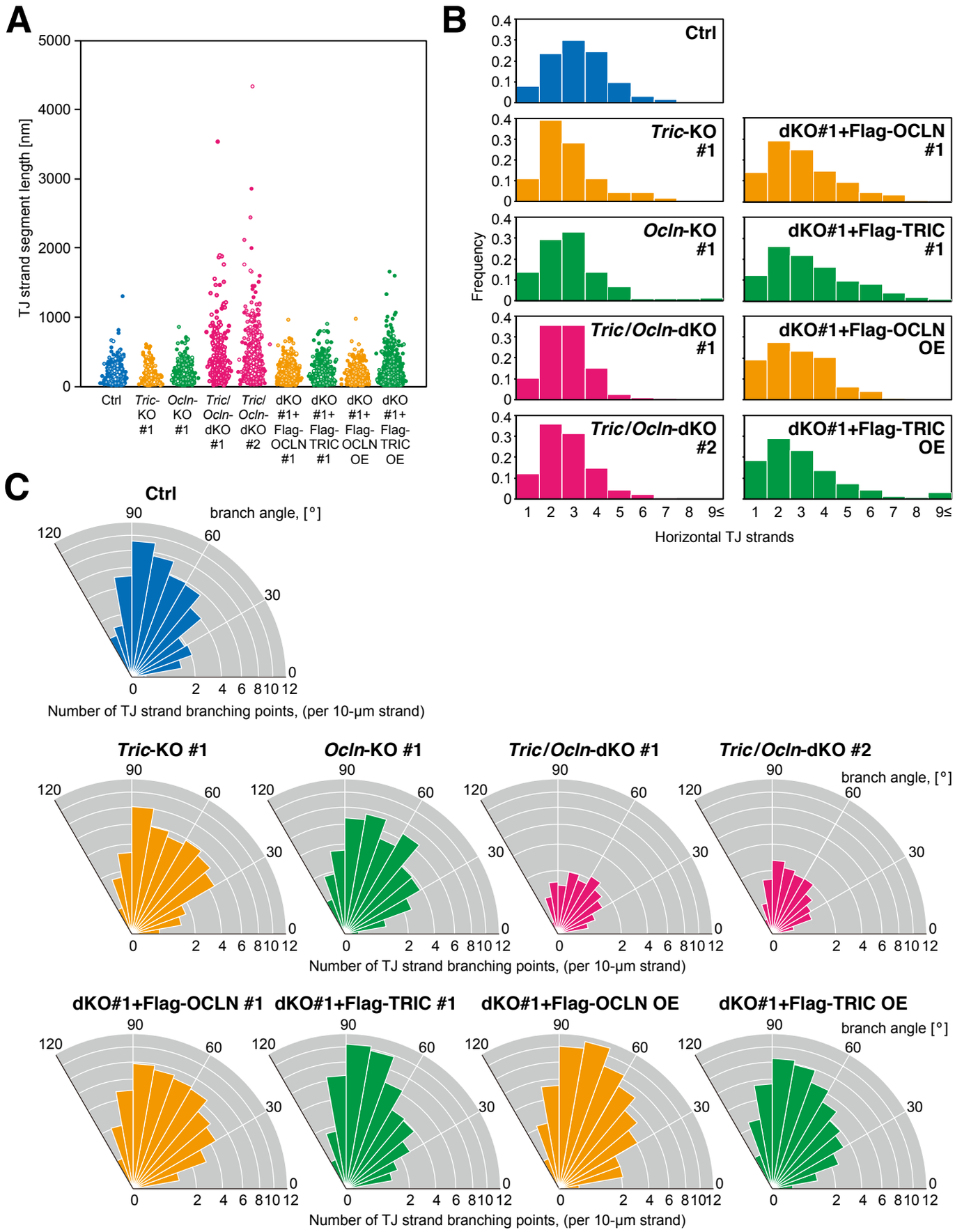

Figure S7. Quantification of the segment length, horizontal strand number and branch angles of TJ strands

(A) The lengths of TJ strand segments are plotted. TJ segments are classified into closed segment (circles filled with dark color), semi-open segment (circles filled with light color) and open segment (open circles).

(B) Distributions of the horizontal TJ strand number are plotted.

(C) The branch angles of TJ strands measured by the method described in Figure S2B were plotted in polar area plots, in which the area of each sector is proportional to the value.

Figure S8

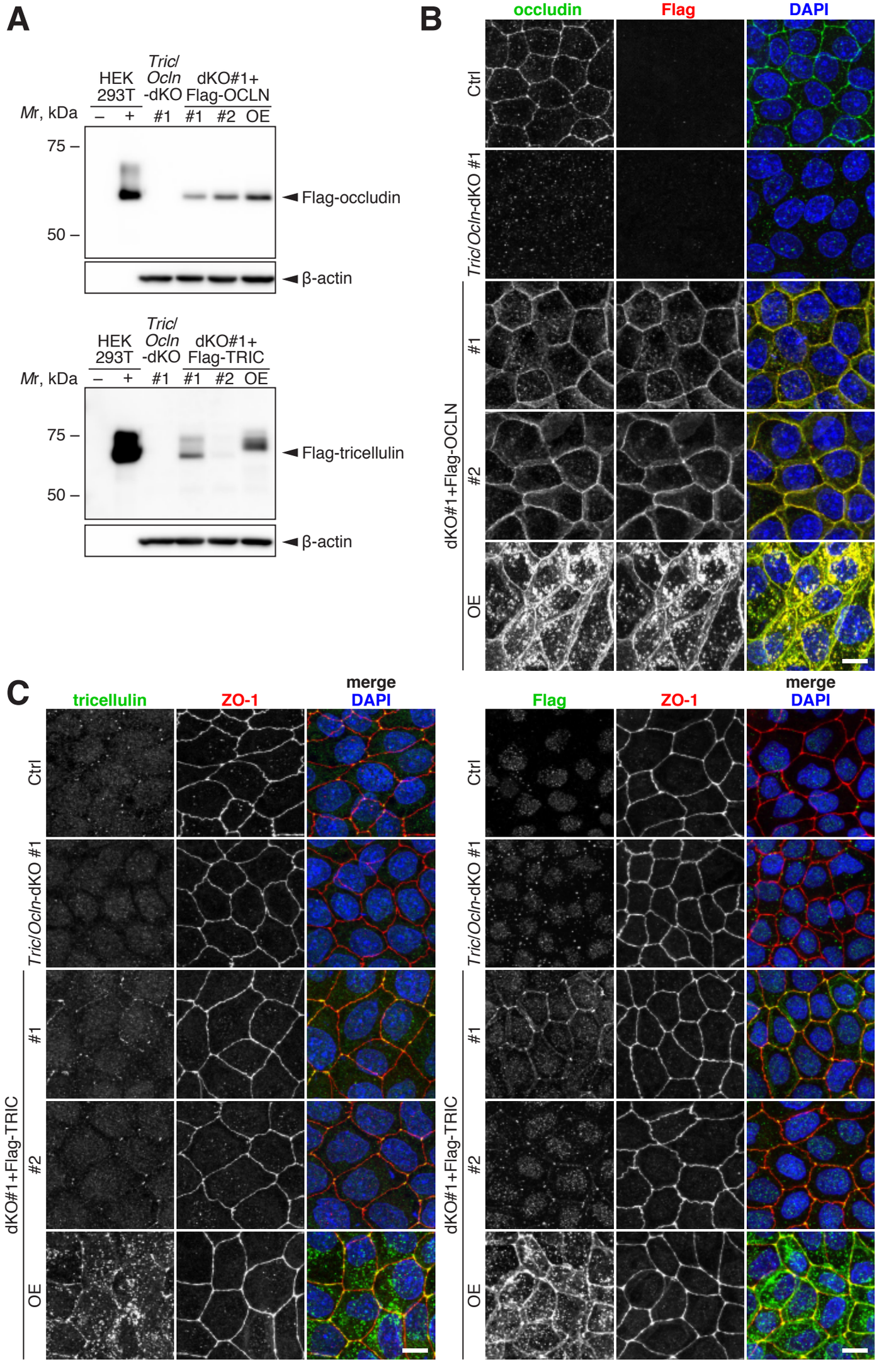
A
HEK 293T
Tric/Ocln -dKO #1
dKO#1+ Flag-OCLN #1
dKO#1+ Flag-OCLN #2
dKO#1+ Flag-OCLN OE
Mr, kDa
75 –
50 –
Flag-occludin
β-actin
HEK 293T
Tric/Ocln -dKO #1
dKO#1+ Flag-TRIC #1
dKO#1+ Flag-TRIC #2
dKO#1+ Flag-TRIC OE
Mr, kDa
75 –
50 –
Flag-tricellulin
β-actin
B
occludin
Flag
merge DAPI
Ctrl
Tric/Ocln-dKO #1
dKO#1+Flag-OCLN #1
dKO#1+Flag-OCLN #2
dKO#1+Flag-OCLN OE
C
tricellulin
ZO-1
merge DAPI
Flag
ZO-1
merge DAPI
Ctrl
Tric/Ocln-dKO #1
dKO#1+Flag-TRIC #1
dKO#1+Flag-TRIC #2
dKO#1+Flag-TRIC OE

Figure S8. Immunoblotting and Immunofluorescence staining of rescue cell lines
(A) Immunoblotting of the total cell lysates of *Tric*/*Ocln*-dKO #1, dKO#1+Flag-TRIC and dKO#1+Flag-OCLN cells with mouse anti-FLAG mAb. HEK293T cell lysates expressing FLAG-tricellulin and FLAG-occludin were used as positive controls. β-actin served as a loading control.
(B) Confocal microscopic images of dKO#1+Flag-OCLN cells. Cells were stained with rat anti-occludin mAb (green), mouse anti-FLAG mAb (red) and DAPI (blue). Scale bar, 20 μm.
(C) Confocal images of dKO#1+Flag-TRIC cells. Cells were double-stained with rat anti-tricellulin mAb (green) and rabbit anti-ZO-1 pAb (red) (left panels), or mouse anti-FLAG mAb (green) and rat anti-ZO-1 mAb (red) (right panels). All cells were stained with DAPI (blue). Scale bars, 20 μm.

Figure S9

A

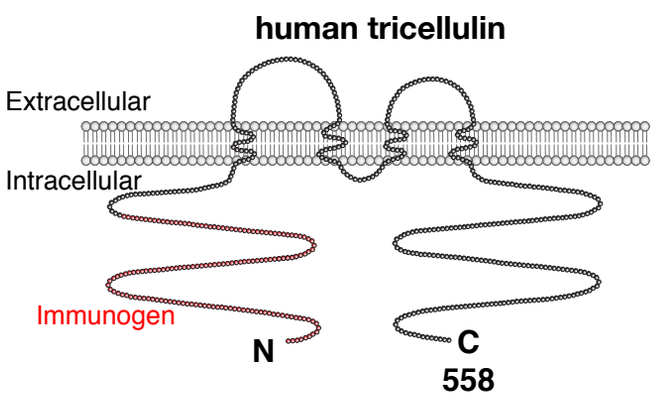

B

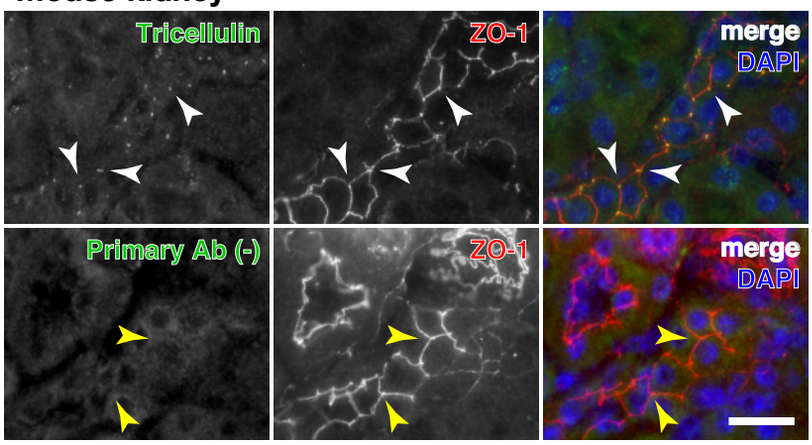

C

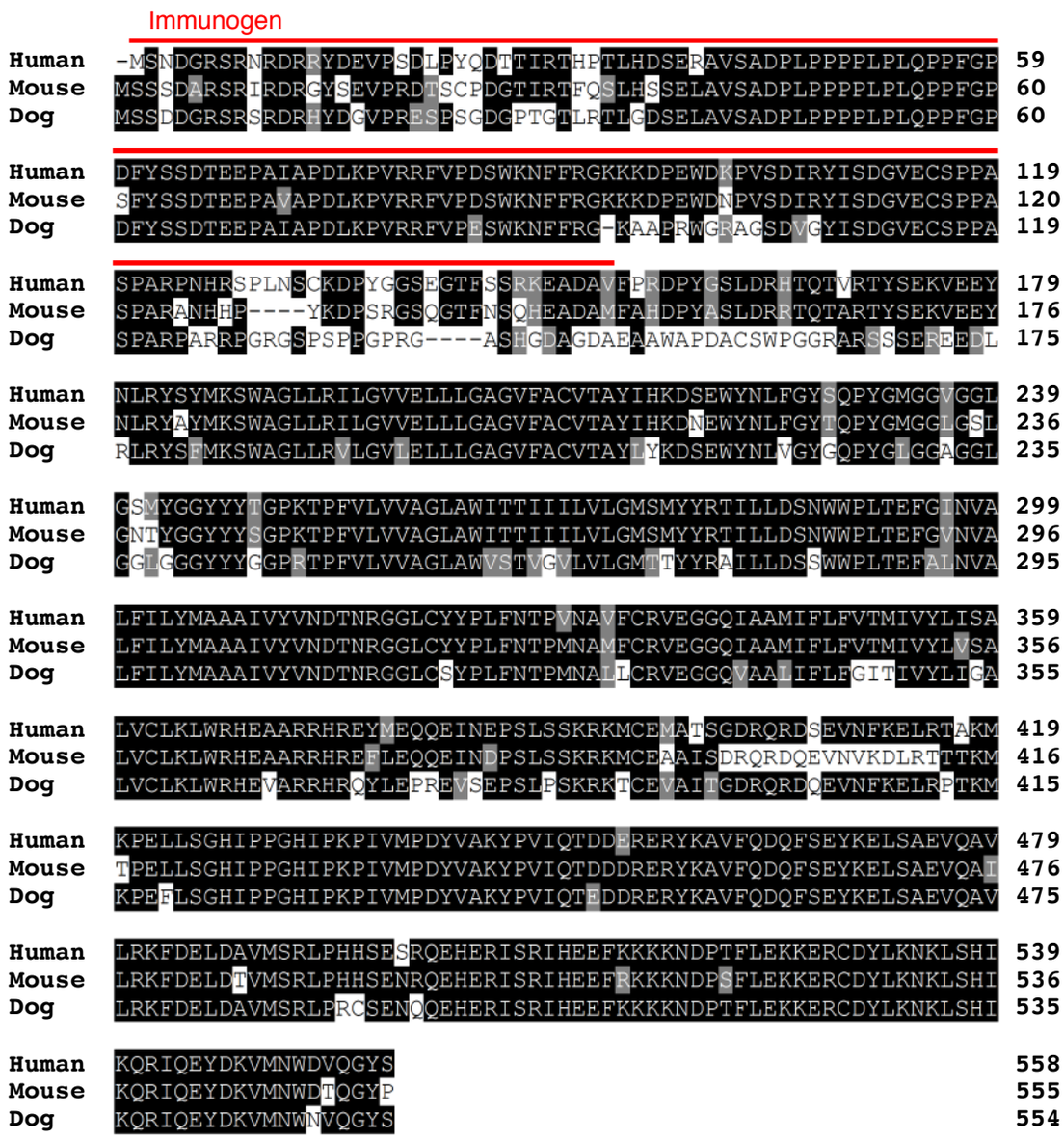

Figure S9. Generation of a rat anti-tricellulin mAb

(A) Schematic diagram of human tricellulin protein. The region used for the immunization of rats to generate the anti-human tricellulin mAb (Clone 1E2) is shown in red (Immunogen).

(B) Characterization of rat anti-tricellulin mAb (1E2) used for immunostaining. Frozen sections of the mouse kidney were immunostained with (upper panels) or without (lower panels) rat anti-tricellulin mAb (green) together with rabbit anti-ZO-1 pAb (red) and DAPI (blue). Note that tricellulin is positive at the tricellular junctions (white arrowheads) of the distal convoluted tubules in the kidney and that treatment with anti-rat secondary antibody alone does not stain the tricellular junctions (yellow arrowheads). Scale bar, 20 μm.

(C) Multiple alignment of amino acid sequences of human, mouse, and dog tricellulin. The red lines indicate the region corresponding to the immunogen.

Table S1. Multiple comparison of TER values and Papp of Ctrl, *Tric*-KO, *Ocln*-KO, *Tric*/*Ocln*-dKO cells, dKO#1+Flag-OCLN, dKO#1+Flag-TRIC cells.
The *p*-values of Tukey-Kramer tests are shown. Pairs with $p < 0.05$ and $p < 0.01$ are filled with light yellow and yellow, respectively.

TER

	Ctrl	*Tric*-KO #1	*Tric*-KO #2	*Ocln*-KO #1	*Ocln*-KO #2	*Tric*/*Ocln*-dKO #1	*Tric*/*Ocln*-dKO #2	dKO#1+ Flag-OCLN #1	dKO#1+ Flag-OCLN #2	dKO#1+ Flag-TRIC#1	dKO#1+ Flag-TRIC#2
Ctrl		0.903	0.000	0.000	0.000	0.000	0.000	0.000	1.000	0.000	0.957
Tric-KO #1			0.002	0.002	0.030	0.000	0.000	0.109	0.902	0.000	0.221
Tric-KO #2				1.000	1.000	0.000	0.000	0.998	0.000	0.883	0.000
Ocln-KO #1					0.999	0.000	0.000	0.997	0.000	0.935	0.000
Ocln-KO #2						0.000	0.000	1.000	0.000	0.471	0.000
Tric/*Ocln*-dKO #1							0.010	0.000	0.000	0.000	0.000
Tric/*Ocln*-dKO #2								0.000	0.000	0.000	0.000
dKO#1+Flag-OCLN #1									0.000	0.468	0.000
dKO#1+Flag-OCLN #2										0.000	0.945
dKO#1+Flag-TRIC #1											0.000
dKO#1+Flag-TRIC #2											

P_{app} of FITC-dextran (4 kDa)

	Ctrl	*Tric*-KO #1	*Tric*-KO #2	*Ocln*-KO #1	*Ocln*-KO #2	*Tric*/*Ocln*-dKO #1	*Tric*/*Ocln*-dKO #2	dKO#1+ Flag-OCLN #1	dKO#1+ Flag-OCLN #2	dKO#1+ Flag-TRIC#1	dKO#1+ Flag-TRIC#2
Ctrl		1.000	1.000	0.941	0.676	0.000	0.000	0.952	1.000	0.158	0.936
Tric-KO #1			1.000	0.988	0.863	0.000	0.000	0.991	1.000	0.320	0.985
Tric-KO #2				0.983	0.836	0.000	0.000	0.987	1.000	0.291	0.979
Ocln-KO #1					1.000	0.000	0.001	1.000	0.999	0.929	1.000
Ocln-KO #2						0.000	0.005	1.000	0.961	0.996	1.000
Tric/*Ocln*-dKO #1							0.233	0.000	0.000	0.000	0.000
Tric/*Ocln*-dKO #2								0.001	0.000	0.104	0.003
dKO#1+Flag-OCLN #1									0.999	0.916	1.000
dKO#1+Flag-OCLN #2										0.501	0.999
dKO#1+Flag-TRIC #1											0.964
dKO#1+Flag-TRIC #2											

P_{app} of FITC-dextran (10 kDa)

	Ctrl	*Tric*-KO #1	*Tric*-KO #2	*Ocln*-KO #1	*Ocln*-KO #2	*Tric*/*Ocln*-dKO #1	*Tric*/*Ocln*-dKO #2	dKO#1+ Flag-OCLN #1	dKO#1+ Flag-OCLN #2	dKO#1+ Flag-TRIC#1	dKO#1+ Flag-TRIC#2
Ctrl		0.866	1.000	1.000	1.000	0.000	0.115	0.999	0.629	0.999	0.992
Tric-KO #1			0.810	1.000	1.000	0.000	0.002	0.471	1.000	0.466	1.000
Tric-KO #2				0.997	0.988	0.006	0.387	1.000	0.582	1.000	0.975
Ocln-KO #1					1.000	0.000	0.050	0.945	0.989	0.943	1.000
Ocln-KO #2						0.000	0.020	0.868	0.995	0.865	1.000
Tric/*Ocln*-dKO #1							0.775	0.025	0.000	0.025	0.000
Tric/*Ocln*-dKO #2								0.715	0.001	0.719	0.020
dKO#1+Flag-OCLN #1									0.266	1.000	0.823
dKO#1+Flag-OCLN #2										0.263	0.999
dKO#1+Flag-TRIC #1											0.819
dKO#1+Flag-TRIC #2											

P_{app} of FITC-dextran (250 kDa)

	Ctrl	*Tric*-KO #1	*Tric*-KO #2	*Ocln*-KO #1	*Ocln*-KO #2	*Tric*/*Ocln*-dKO #1	*Tric*/*Ocln*-dKO #2	dKO#1+ Flag-OCLN #1	dKO#1+ Flag-OCLN #2	dKO#1+ Flag-TRIC#1	dKO#1+ Flag-TRIC#2
Ctrl		0.997	1.000	0.995	1.000	0.808	0.992	0.834	0.998	0.744	0.996
Tric-KO #1			0.999	1.000	1.000	1.000	1.000	0.999	1.000	0.997	1.000
Tric-KO #2				0.999	1.000	0.911	0.998	0.917	0.999	0.858	0.999
Ocln-KO #1					1.000	1.000	1.000	1.000	1.000	0.999	1.000
Ocln-KO #2						0.996	1.000	0.996	1.000	0.987	1.000
Tric/*Ocln*-dKO #1							1.000	1.000	1.000	1.000	1.000
Tric/*Ocln*-dKO #2								1.000	1.000	1.000	1.000
dKO#1+Flag-OCLN #1									1.000	1.000	1.000
dKO#1+Flag-OCLN #2										0.998	1.000
dKO#1+Flag-TRIC #1											1.000
dKO#1+Flag-TRIC #2											

Table S2. Primers used for genomic PCR in this study.

Name	Gene locus	Sequence
Primer F_C2	*Cldn2*	5’-GATGCCTTCTTGAGCCTGCTTGTGG-3’
Primer R_C2	*Cldn2*	5’-AGCACCTTCTGACATGATACAGTGC-3’
Primer-A	*Tric*	5’-CACCGTCCCAAGGGAGTCCCCGTC-3’
Primer-B	*Tric*	5’-AAACCAGGACCGCCTGGACTTCGG-3’
Primer-C	*Tric*	5’-AAACCTCCGTCCGAGATGTACCCG-3’
Primer-D	*Ocln*	5’-CACCCCGAGCAATGATGTGTACGG-3’
Primer-E	*Ocln*	5’-CCTCTTGGGGATCTACCACACAGTA-3’

Video 1. Computational simulation of continuous flow of macromolecules through broken TJ strands in simplified TJ network model

Image sequences of typical heat map of macromolecular concentrations (4 kDa) in each compartment from 0–7200 [sec] in the three-horizontal-row model. The movie in the order from top to bottom indicates partition density = 0, 1.2, 4.4 and 10 μm^{-1}, respectively. The display sizes of donor and acceptor were reduced. The images were constructed using Matlab's (command "heat map"), were animated using ImageJ software ("Import"-"Image Sequence"), and were converted to mp4 filename extension using FFmpeg.